https://doi.org/10.3311/PPme.18691

Periodica Polytechnica Mechanical Engineering, 65(4), pp. 385–397, 2021

Chromatic Discrimination Thresholds as a Function of Color Differences and Cone Excitations

Ágnes Urbin[1*], Balázs Vince Nagy[1]

[1] Department of Mechatronics, Optics and Mechanical Engineering Informatics, Faculty of Mechanical Engineering, Budapest University of Technology and Economics, H-1111 Budapest, 4-6. Bertalan Lajos Str., Hungary
[*] Corresponding author, e-mail: urbin@mogi.bme.hu

Received: 01 June 2021, Accepted: 21 July 2021, Published online: 21 September 2021

Abstract

In this paper, Just Noticeable Differences (JNDs) of color-normal subjects measured towards the Protan, Deutan, and Tritan confusion points are presented as a function of the chromaticity of the reference points. Measurements were executed with the Cambridge Colour Test Trivector test in equidistant reference points towards eight directions equally spaced and centered on the neutral reference point in the CIE 1976 UCS diagram.

Results were evaluated as the function of the distance between the reference points and the neutral point. The reference points were the chromaticities of the backgrounds of the pseudoisochromatic plates in the test, and the neutral point was defined as equal energy white. The evaluation was performed considering $\Delta E_{u'v'}$ differences and $L/(L+M)$ and $S/(L+M)$ ratios of the cone-excitations.

Chromatic discrimination thresholds exceeded the normative upper limit of color normal subjects in $\Delta E_{u'v'}$ units at extreme reference points. Shifting the reference points from the neutral point towards the confusion points indicated an increase of Just Noticeable Differences measured towards the confusion points following second-order polynomials. Based on our results a model estimating the JNDs expressed in $\Delta E_{u'v'}$ units towards the confusion points was recommended.

Even though CIE 1976 UCS diagram is not a perceptually uniform color space, the Just Noticeable Differences measured with the CCT correlate with the corresponding L' and S' cone excitations. This confirms the basic applicability of the CIE 1976 UCS diagram for characterizing Just Noticeable Differences. For complete perceptual analysis, the use of cone-excitation-based metrics is still essential and recommended.

Keywords

chromatic discrimination, discrimination thresholds, cone excitations, Just Noticeable Differences (JNDs)

1 Introduction

A prevalent way to answer research questions regarding color vision is observing chromatic discrimination ability, which may be quantified by measuring Just Noticeable Differences (JNDs). JNDs can be understood as the thresholds of chromatic discrimination, in other words, the inverse of the sensitivity of color discrimination [1].

Discrimination thresholds can be measured in different dimensions such as light levels, wavelength ranges, or chromaticity coordinates [2, 3]. In measuring thresholds in terms of chromaticity, the physiological properties of the applied chromaticity diagram are essential.

The chromaticity diagram proposed by MacLeod and Boynton [4] is widely used to represent perceived chromaticity and to evaluate physiological tests [5–7]. The MacLeod-Boynton diagram shows cone excitation by equiluminant stimuli in terms of the signals of the two physiological pathways: $L/(L+M)$ against $S/(L+M)$, where L, M, and S represent the excitations of the long-, middle-, and short-wavelength sensitive cones, respectively. These axes were later on noted as "cardinal" axes [8].

A fundamental measurement of JNDs in terms of chromaticity was carried out and published first by MacAdam [9]. A filtered light source generated stimuli, and the JNDs were calculated from the standard deviation of the results of color matching tasks. Even though results were plotted in the CIE 1931 xyY chromaticity diagram, MacAdam's experiment provided data for analyses of chromaticity measurements in cone-excitation spaces. A classical analysis of LeGrand interpreted MacAdam's data in terms of coneexcitations [10, 11] and concluded that in the

Cite this article as: Urbin, Á., Nagy, B. V. "Chromatic Discrimination Thresholds as a Function of Color Differences and Cone Excitations", Periodica Polytechnica Mechanical Engineering, 65(4), pp. 385–397, 2021. https://doi.org/10.3311/PPme.18691

case of pure chromatic differences, only the two physiological dimensions corresponding to the two dimensions of the chromaticity plane need to be analyzed [2]. Another analysis published by Nagy et al. [12] confirmed Le Grand's conclusions with analysis based on extended data.

Although many studies can be found interpreting experimental results of JNDs, even contradictions can be found among the results and the conclusions. Contradictions can be understood since chromatic discrimination strongly depends on experimental conditions, such as the stimuli, the field of view, the state of adaptation, the reference white, or the luminance [13]. The complexity of these correspondences requires prudence regarding the experimental design, measurements, and the analysis and publication of results. Although analysis based on cone-excitations provides physiologically helpful information, it is also prevalent to find the CIE chromaticity diagrams such as the CIE 1931 *xyY* chromaticity diagram (representing the *xy* chromaticity plane at a luminance (*Y*) level), the CIE 1976 uniform-chromaticity-scale diagram, or the 1976 *L*a*b** color space as the base of experimental design and analysis.

In measuring chromatic discrimination, the following parameters must be precisely defined: the field of view, the luminance, and the spectral content (or chromaticity) – each regarding both the reference and the target stimulus.

A well-known method to avoid luminance mechanisms in color vision research is applying pseudoisochromatic tests. Pseudoisochromatic tests have two main components: the figures and the algorithm.

Pseudoisochromatic figures in general consist of dots of random size and luminance on a uniform disk. All dots vary in luminance, and dots are grouped as reference and target, differing in chromaticity. The task is to discriminate the target from the reference. Discrimination can be confirmed in various ways, such as identifying characters or the orientation of symbols or in dynamical implementations by following movements. The correct answer indicates that the subject can discriminate the actual target from the reference. Therefore, the perceived difference between them is higher than the subject's Just Noticeable Difference.

Therefore, the reference pattern and the target are the main characteristics of the figure, which define the actual observed quantity: the perceptible difference between them.

Algorithms correspond with the aim of the actual test: if the objective is to identify a particular group of subjects, it is enough to count the scores collected for each figure and decide if the subject reached the criteria. An example of this case is the Ishihara test [14], a paper-based test designed for identifying anomalous trichromacy. The task is to read numbers, and in case the subject does not reach the expected number of correct answers, the subject can be considered an anomalous trichromat.

In another type of measurement, the aim is to approximate the exact value of the discrimination threshold. In this case, paper-based tests with printed figures give limited opportunity, while computer-based tests are beneficial because of the application of adjustable stimuli and dynamic algorithms. A widely used example for this type of measurement is the Cambridge Colour Test (CCT), a computerized pseudoisochromatic test [15, 16] measuring JNDs towards assigned directions from the reference chromaticity point in the CIE 1976 UCS diagram [17].

In the case of CCT the target is a Landolt-C character, shown in Fig. 1. The target is randomly presented in one of four orientations while the task is to detect the orientation of the character. Therefore, the field of view most relevant to the target is the angle under which the gap of the Landolt-C character is seen. In case the gap is seen under 1°, the outer diameter of the Landolt-C character is seen under 4.3° and the inner diameter is seen under 2.2° [18]. Binocular summation does not affect color discrimination thresholds of normal color observers measured with CCT, therefore results of CCT measurements obtained monocularly and binocularly can be analyzed together [19].

The native color space of the CCT is the CIE 1976 UCS diagram, therefore the chromaticity of the reference and the target is defined as (u';v') coordinates. During a test procedure the reference chromaticity is constant while the target chromaticity varies towards the reference

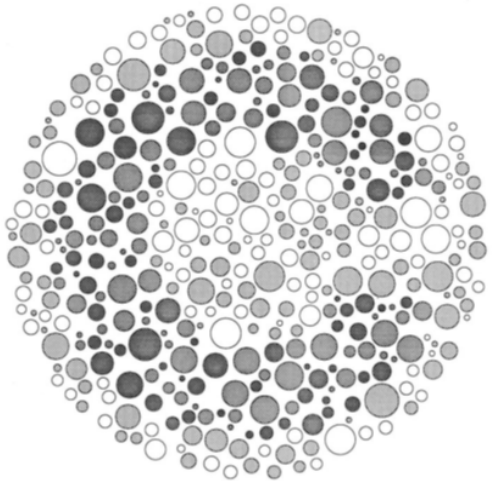

Fig. 1 The test figure of the Cambridge Colour Test (CCT) demonstrating the relative sizes of the target and the background [18]. The target is demonstrated with darker dots compared to the reference.

chromaticity in the UCS diagram following a staircase protocol based on the answers of the subject: after a right answer the distance is decreased, and in case of a wrong answer the distance is increased by the algorithm.

The uniform disk behind the reference and target dots is dark and achromatic while the pseudoisochromatic test-figures are displayed. Between two test-figures the disk appears in the chromaticity of the actual background chromaticity for 1 sec. The luminance of the dots is individually randomized in predefined range and levels [15, 17].

Regarding the measurement directions there are two options of the CCT: the Ellipse Test and the Trivector Test. In the Ellipse Test measurement directions are equidistant directions around the reference point. Besides the actual JNDs, the result is an ellipse fitted with the least-squares method estimating the area in which the subject cannot discriminate chromaticity. In the Trivector test, there are three measurement directions, defined by the reference point and the (Protan, Deutan, and Tritan) confusion points. Both the Ellipse and the Trivector test are pretty effective for screening anomalous trichromacy, while the chromatic resolution of the ViSaGe MKII system allows us to screen differences even between normal color observers.

Normative values for JNDs measured with the CCT are available in terms of different age groups [20–22] or different color-vision abilities [23, 24]. However, these normative results generally represent data measured close to the neutral reference point that compares different groups of subjects.

No normative data was found in the literature regarding CCT results in reference points providing information about the perceived chromaticity diagram as a whole.

Our experiment aimed to describe chromatic discrimination characteristics depending on the reference (background) color. We measured chromatic discrimination thresholds of normal color observers in 66 reference points covering the whole gamut of a display. The locations of the reference points are later detailed in Subsubsection 2.4.2 as part of the experimental design. The JNDs were observed towards the Protan, Deutan, and Tritan confusion lines; hence our results describe the *L*, *M*, and *S* cone responses separately.

Results were interpreted both in the CIE 1976 UCS diagram and in a cone excitation space based on the Stockman and Sharpe [25] 2° cone fundamentals.

2 Methods

In the experiment, JNDs of color-normal subjects were measured with the Cambridge Colour Test Trivector module comprising a sequence of pseudoisochromatic plates. Our results were evaluated in reference to the reference chromaticity of the CCT (therefore, the chromaticity of the background dots of the pseudoisochromatic figures).

2.1 Equipment

A MultiSync® FP2141SB™ Display with 20 inches diagonal image size (1600 × 1200 pixels) was used to display stimuli controlled with ViSaGe MkII. Gamma correction was performed with a ColorCAL MkII colorimeter (Cambridge Research System).

2.2 Stimulus

The pseudoisochromatic figures were displayed full screen. The diameter of the whole stimulus was 11.7 inches. The viewing distance was 3 meters providing that the gap of each Landolt-C figure was shown under 1° visual angle. The luminance of each dot was randomly selected from 6 levels between 2 and 8 cd/m^2. Fig. 2 shows Fairchild's viewing conditions demonstrating the field sizes applied in the color appearance models defined by the CIE, merged with the CCT figures in our experiment. It can be concluded that the screen and the test figures filled the field of view dedicated to the stimulus.

2.3 Subjects

A total of 78 color-normal subjects (22.8 ± 1.4 years old) participated in the study. Normal color vision of the subjects was validated by their Trivector results measured in the neutral reference point. Subjects were not considered color-normals, and they were excluded from the experiment if their measured JNDs in terms of $\Delta E_{u'v'}$ exceeded 100 × 10^{-4} towards either the Protan or the

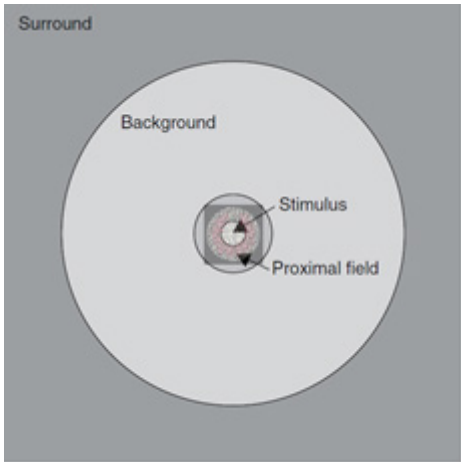

Fig. 2 Demonstrating the magnitude of the field of view of the CCT test figure compared to the viewing conditions applied in the CIE color appearance models [1].

Deutan confusion point or 150 × 10^{-4} towards the Tritan confusion point [17].

The experiments were approved by the United Ethical Review Committee for Research in Psychology (EPKEB, Hungary, reference number: 04/2016). All subjects signed written consent, agreeing to participate in the measurements after verbal and written orientation.

2.4 Experimental design

Input and output chromaticity coordinates (u';v') and the measured discrimination thresholds ($\Delta E_{u'v'}$) presented in this paper are interpreted in the CIE 1976 UCS diagram, following the definitions of the CCT manual [17].

Our experimental design followed the main parameters of the CCT Trivector test: the chromaticity coordinates of the reference points, the chromaticity coordinates of the confusion points, the range, and the number of levels of the luminance noise over the pseudoisochromatic plates.

2.4.1 Control variables

Display luminance levels were reduced to the range between 2 and 8 cd/m^2, differing from the values recommended in the CCT manual [17]. The reduction was to provide a broader gamut to increase the number of visualized reference points. Luminance levels were selected in 6 levels as the default setting of the CCT.

Confusion points were fixed to the following (u';v') chromaticity coordinates: Protan (0.6579;0.5013), Deutan (−1.2174;0.7826), Tritan (0.2573;0.0000). The neutral point was defined as the chromaticity of the equal energy white: (0.2024;0.4684).

2.4.2 Independent variables

The systematically manipulated independent variables were the reference points. Reference chromaticities were equidistant points towards eight directions (further on noted as reference directions) equally spaced and centered on the neutral point in the CIE 1976 UCS diagram, covering the display's gamut. The 66 reference points and the reference directions labeled from (0) to (7) are shown in Fig. 3.

Reference points were labeled with ordinal numbers towards each reference direction. The neutral point was always labeled as 0, and ordinal numbers increased towards the arrows of directions shown in Fig. 3. These ordinal numbers were later used during analysis as the argument.

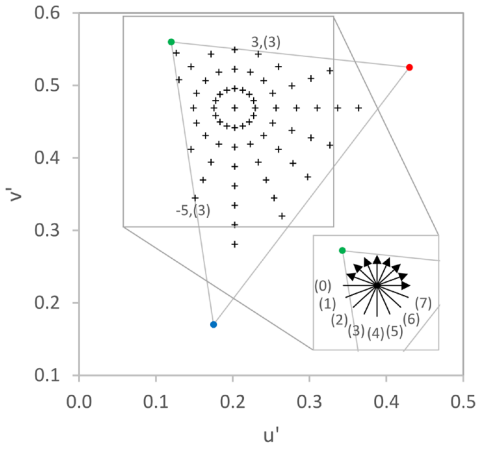

Fig. 3 Gamut of the display and the 66 reference points equally spaced with $\Delta E_{u'v'} = 0.027$ along with the eight directions centered on the neutral point, covering the gamut of the display. The eight directions (further on noted as reference directions) are labeled from (0) to (7), as shown in the bottom right corner. Reference points −5 and 3 along reference direction (3) are labeled.

2.4.3 Dependent variables

As the measured quantity, the JNDs towards the Protan, Deutan, and Tritan confusion lines (further on **P**, **D**, and **T** values) were the dependent variables.

2.4.4 Confusion lines

The relation between the reference directions and the confusion lines originating from the neutral point should be observed.

As Fig. 4 shows, Protan confusion line approximates reference direction (0), Deutan confusion line runs between reference directions (7) and (0), while Tritan confusion line approximates reference direction (4).

As the abscissa of the Deutan confusion point is negative, in the CCT trivector test, Deutan direction is mirrored

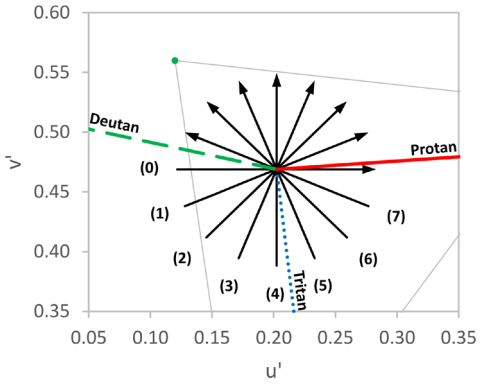

Fig. 4 The reference directions and the confusion lines originating from the neutral point

to the reference point and measured along with the confusion line but towards the increasing abscissas.

Since confusion points were fixed and reference points varied in the experiment, the direction towards the confusion points from the reference point (further on noted as measurement directions) varied with the reference points, as shown in Fig. 5.

In the three reference directions, which approximate the confusion lines ((0), (4), and (7) in Fig. 4), the JNDs may be mainly interpreted as saturation differences. In the other reference directions, the JNDs may have a component of hue changes towards the chromaticities of the confusion points (see Fig. 5).

2.4.5 Within-subjects and between-subjects design

The experiment was composed of a combination of within-subjects and between-subjects design. In the between-subjects design, four sets of reference points were considered. In each set, the reference points of perpendicular pairs of reference directions were grouped. Combining perpendicular reference directions instead of adjacent reference directions was to distribute the effect of directions along with the gamut. The four sets were the following: Set I. (reference directions (0) and (4)) consisted of 20 reference points; Set II. (reference directions (1) and (5)) consisted of 18 reference points; Set III. (reference directions (2) and (6)) consisted of 17 reference points; Set IV. (reference directions (3) and (7)) consisted of 18 reference points as shown in Fig. 6.

The neutral point was included in each set to compare the results of the four sets of measurements.

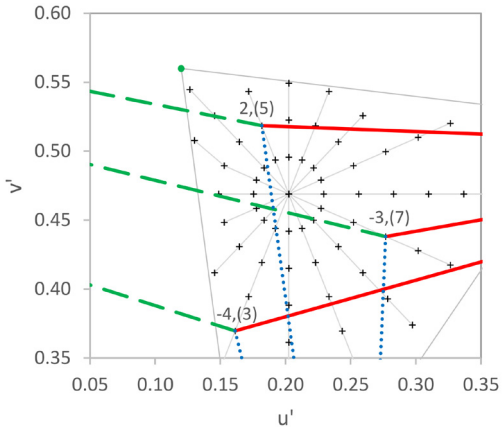

Fig. 5 The Protan (solid), Deutan (dashed), and Tritan (dotted) confusion lines directed from reference point −4 on reference direction (3) (bottom), reference point −3 on reference direction (7) (middle), and reference point 2 on reference direction (5) (top).

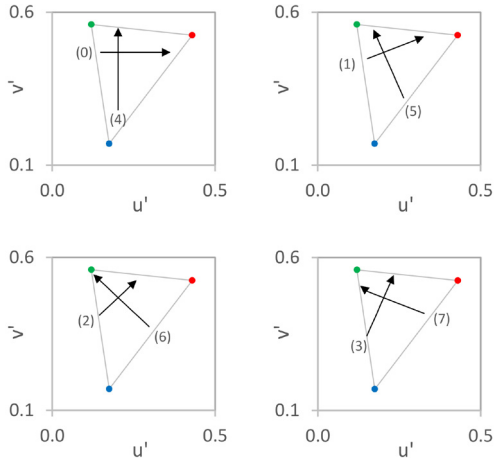

Fig. 6 The four sets of reference points grouped in the between-subjects design. Reference points of perpendicular reference directions were grouped as Set I: (0) and (4), top left; Set II: (1) and (5), top right; Set III: (2) and (6), bottom left and Set IV: (3) and (7), bottom right.

Each set of measurements was considered as a within-subjects design. Subjects accomplished the CCT Trivector test in each reference point with no repetition. Reference points were selected in a randomized order. A total of 20 subjects accomplished the measurements in each set.

Subjects were invited to participate in a single set of measurements; however, involvement in more sets was also allowed. Two subjects accomplished two sets of measurements; therefore, the 78 subjects accomplished the 80 sets of measurements.

2.5 Procedure

Measurements were performed binocularly in a dark room. Before measurements, two minutes were provided for dark adaptation while instructions were explained.

Subjects had to detect the orientation of pseudoisochromatic Landolt-C figures in sequences using a controller with four keys. Test images were shown until response, but for 3 seconds at the longest. In the test sequence between two test images, the uniform background disk without the pseudoisochromatic figure was displayed for 0.5 second in the chromaticity of the actual reference chromaticity.

Accomplishing one set of measurements took approximately one hour, including dark adaptation, prior instructions, trial tests, the main test sequence, and short breaks.

3 Experimental results and analysis

Results were analyzed both in the CIE 1976 UCS diagram and in terms of cone excitations.

3.1 Results in terms of $\Delta E_{u'v'}$ color differences

The results of the measurements are shown in Figs. 7 and 8. The diagrams show the average JNDs and standard deviations towards the Protan, Deutan, and the Tritan confusion points (**P**, **D**, and **T** values) in the function of reference point locus in the CIE 1976 UCS diagram. Dotted lines show second-order polynomials fitted to the data detailed later in Subsubsection 3.1.4.

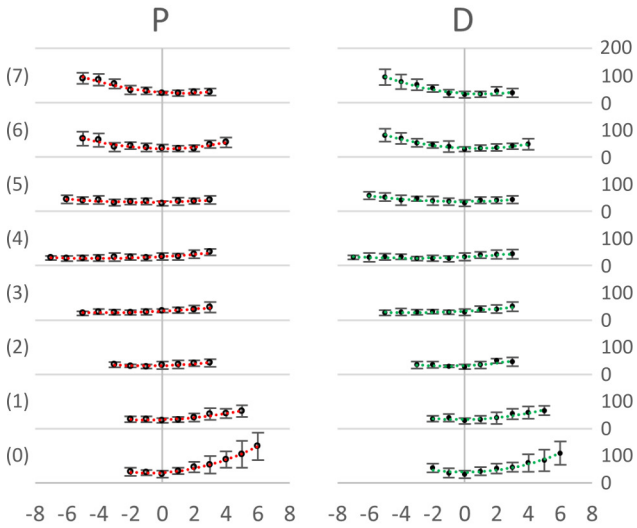

Fig. 7 The means and standard deviations (±1 SD) of the measured JNDs towards the Protan and Deutan confusion points as a function of the reference point location in the CIE 1976 UCS diagram. The abscissa is the ordinal number of reference points, as explained in the description of the experimental design. Data is shown for reference directions from (0) to (7) following the left ordinates. The right ordinates represent the distances within the CIE 1976 UCS diagram multiplied by 10^4. The scales of the subplots are 0–200.

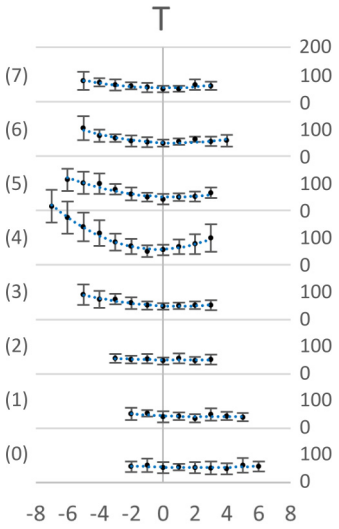

Fig. 8 The means and standard deviations (±1 SD) of the measured JNDs towards the Tritan confusion point as a function of the reference point location in the CIE 1976 UCS diagram. The abscissa is the ordinal number of reference points, as explained in the description of the experimental design. Data is shown for reference directions from (0) to (7) following the left ordinates. The right ordinates represent the distances within the CIE 1976 UCS diagram multiplied by 10^4. The scales of the subplots are 0–200.

Upper limits for color normal subjects in the CCT Trivector test published in the CCT manual are 100×10^4 (Protan and Deutan) and 150×10^4 (Tritan) [17]. A study observing normal color observers from a range of age like our subjects (18 to 30 years old), interpreted even lower thresholds: 70×10^4 (Protan), 85×10^4 (Deutan) and 115×10^4 (Tritan) [26]. **P** and **D** values approximate in reference direction (6) and (7) and exceed in reference direction (0) even the higher published upper limit within the range of reference points. **T** values exceed the corresponding (higher) upper limit in reference direction (4) and approximate in reference direction (3), (5), and (6) (see Figs. 7 and 8).

3.1.1 Comparing results measured in the neutral point

Datasets were corrected to a normal distribution with excluding outliers. However, since variances were unequal, Student's *t*-test was not appliable, so Welch's unequal variances *t*-test was applied to compare the results measured in the neutral reference point in different sets of measurements (I, II, III, IV) to compare the results of the between-subjects approach.

Welch's tests were evaluated pairwise for each combination. Since *p*-values were higher than 0.05 in each case, we did not see the reason to conclude that there were significant differences between the results of subjects participating in the four different sets of measurements. Therefore between-subjects results were pooled in the evaluation.

3.1.2 Correlation between P-D, P-T, and D-T datasets

Figs. 7 and 8 indicate a strong relationship between Protan and Deutan data; therefore, correlation analysis was executed.

Fig. 9 shows the scatter plot of the average JNDs measured towards the Protan and the Deutan confusion points in each reference point. The scatterplot of the pooled data shows a strong, positive, linear relationship between the chromatic discrimination thresholds measured towards the Protan and the Deutan directions. The strength and the significance of the relationship vary in the different measurement directions. Spearman's correlation coefficients and the corresponding *p*-values between the averages of the datasets in **P-D**, **P-T**, and **D-T** combinations, towards the 8 measurement directions are shown in Table 1.

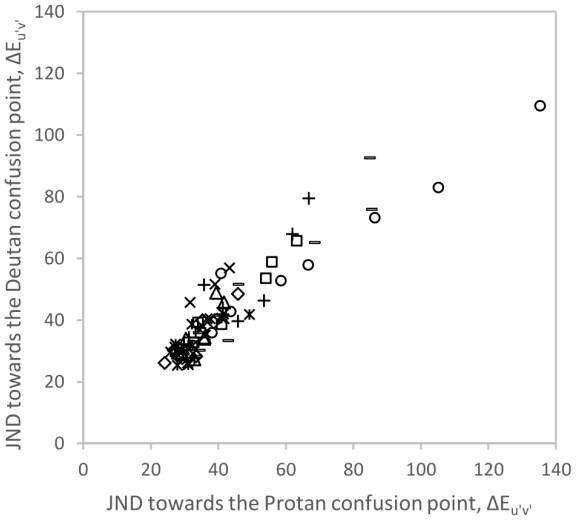

Fig. 9 Scatter plot of the average JNDs measured towards the Protan and the Deutan confusion points in each reference point. Different markers show data corresponding to the eight measurement directions.

Table 1 Spearman correlation coefficients and *p*-values describing the relationship between the average JNDs

	Protan Deutan		Protan Tritan		Deutan Tritan	
	Corr. coeff.	*p*-value	Corr. coeff.	*p*-value	Corr. coeff.	*p*-value
(7)	0.90	0.0009	0.78	0.0125	0.93	0.0002
(6)	0.88	0.0008	0.64	0.0479	0.85	0.0016
(5)	0.60	0.0667	0.68	0.0289	0.81	0.0289
(4)	0.52	0.0800	-0.43	0.1667	0.05	0.8799
(3)	0.73	0.0246	-0.62	0.0769	-0.28	0.4600
(2)	0.83	0.0212	-0.18	0.7017	-0.02	0.9694
(1)	0.93	0.0009	-0.17	0.6932	0.02	0.9554
(0)	0.95	0.0001	0.10	0.7980	0.15	0.7001

3.1.3 Effect of the reference point

To find if the chromaticity of the reference point has a significant effect on JNDs, raw data measured in each reference point was compared with the data measured in the neutral reference point using Welch's test.

Fig. 10 shows the boundaries of the approximated areas in which the Welch test did not show significant differences with the results measured in the neutral point for **P**, **D**, and **T** values ($p > 0.01$).

The intersection of the three areas covers the reference points in which JNDs did not change significantly towards any confusion lines.

3.1.4 Estimation of JNDs

Figs. 7 and 8 indicate that the reference point's shift towards the measurement direction indicates the increase of the JNDs.

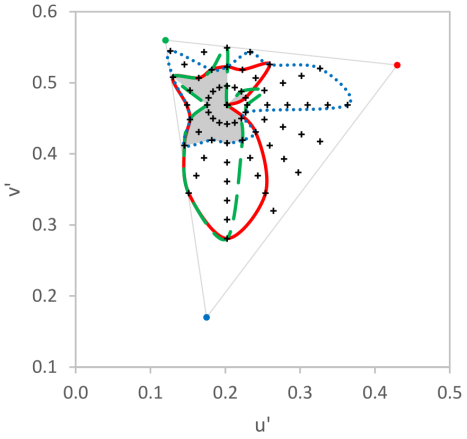

Fig. 10 The boundaries of the approximated areas in which no significant difference ($p > 0.01$) was found with Welch's test in the **P** (solid), **D** (dashed), and **T** (dotted) values compared to the results measured in the neutral point. The intersection of the three areas is filled with grey.

Control measurements were executed to observe the effect of saturation in reference directions (3) and (5) towards the blueish chromaticities. JNDs were measured towards the saturated blueish chromaticities following the reference directions instead of the Tritan confusion line. Detailed analysis was not executed, but initial results did not show similar increases in JNDs, proposing that the increase is most likely caused by the shift towards the confusion points than pure saturation discrimination.

To extend these observations to a continuous form, second-degree polynomial functions were fitted to the datasets. The polynomial functions defined as Eq. (1) are shown in Figs. 7 and 8 with dotted curves.

$$y = c_2 \left(x - x_0\right)^2 + c_0 \tag{1}$$

The c_2 coefficients were analyzed in terms of the reference directions ($\delta_i = i \times \pi/4$; $i = 0$ to 7) for each three measurement directions. To approximate the distribution of the coefficients, ellipses were fitted with the least-square method. The ellipses were defined in the form of Eq. (2), as seen in Fig. 11:

$$r(\theta) = \sqrt{\frac{a^2 + b^2}{a \times \sin^2(\theta) + b \times \cos^2(\theta)}}, \tag{2}$$

where:

- r denotes the dependent variable,
- θ denotes the argument,
- a denotes the radius on the major axis,
- b denotes the radius on the minor axis, and
- ϑ denotes the angle of the major axis and the abscissa.

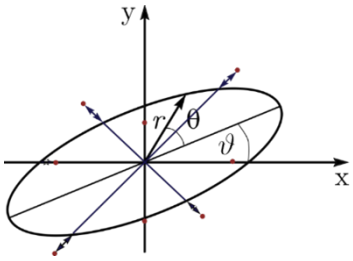

Fig. 11 Demonstration of the parameters for the ellipse-fitting using the least-squares method

Fig. 12 shows the c_2 coefficients and the fitted ellipses in terms of the reference directions for each measurement direction. Data points were mirrored to the $[\pi;2\pi]$ interval only for demonstration.

The parameters of the ellipses are given in Table 2. Protan and Deutan results are similar while Tritan results show different pattern as expected from Figs. 7 and 8.

In Fig. 13 the ellipses from Fig. 12 are plotted on the CIE 1976 UCS diagram, centered to the neutral reference point. It demonstrates that the major axes of the ellipses fitted for the Protan and Deutan data approximate the bicentric of the Protan and Deutan confusion lines, while the major axis of the ellipse fitted to the Tritan data approximates the Tritan confusion line.

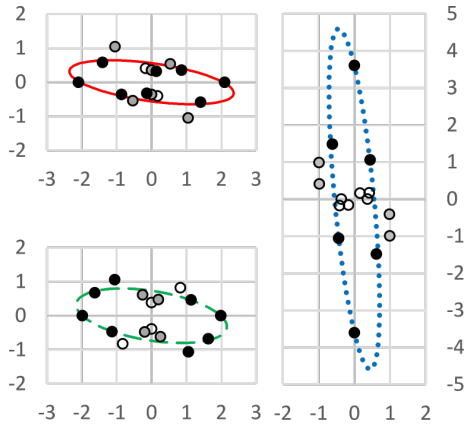

Fig. 12 The c_2 coefficients and the fitted ellipses in terms of the reference directions ($\delta_i = i \times \pi/4$; $i = 0$ to 7) for the Protan (left, top), the Deutan (left, bottom), and the Tritan (right) measurement directions. The markers are filled corresponding to the coefficients of determination of the second degree polynomial functions from which c_2 values were derived: black fill: $0.9 \le R^2$; grey fill: $0.8 \le R^2 \le 0.9$ and no fill: $R^2 \le 0.8$.

Table 2 The parameters of the ellipses defined in Eq. (2): a denotes the radius on the major axis, b denotes the radius on the minor axis, and ϑ denotes the angle of the major axis and the abscissa.

	Protan	Deutan	Tritan
a	2.3810	2.1872	4.6203
b	0.5549	0.7254	0.5507
ϑ	171.84°	170.62°	95.57°

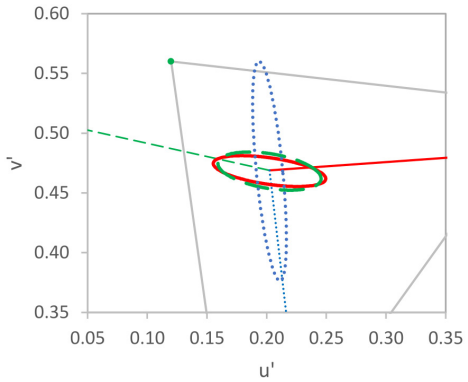

Fig. 13 The confusion lines and the fitted ellipses from Fig. 12 plotted on the CIE 1976 UCS diagram

Fig. 13 and Table 2 confirm the assumption that c_2 coefficients increase towards the actual measurement directions.

Measurement directions (5), (6) and (7), run between the major axes of the fitted ellipses (see Figs. 4 and 13). In these directions the superposition of the effects of all three confusion lines might explain the correlation between **P-T** and **D-T** datasets (see Table 1).

In each measurement direction x_0 values were in the intersection area shown in Fig. 10, indicating that there was no significant difference between the local minimum of the second-degree polynomial functions (c_0) and the JNDs measured in the neutral reference point. As a confirmation, Welch's tests were executed between these values pooling all reference directions towards each measurement direction, and the results showed no significant difference between the three pairs of groups.

As conclusion, x_0 can be estimated with 0 and c_0 can be estimated with JND values measured in the neutral reference point.

3.2 Results in terms of cone excitations

Results expressed in $\Delta E_{u'v'}$ should not be compared in terms of discriminability without acknowledging that the CIE 1976 UCS diagram is not a perceptually uniform color space [27].

To clarify if the source of the increased thresholds is the non-uniformity of the native color space or not, results were evaluated in terms of cone excitations.

3.2.1 Results plotted in the MacLeod-Boynton diagram

Chromaticity points related to the JNDs were calculated: P, D, and T points were measured at the distance of the corresponding average JNDs towards the confusion points. Calculations were executed in each reference point. Note that P, D, and T points are the chromaticity points of the Landolt-C figures at the measured thresholds, not to be

confused with the Protan, Deutan, and Tritan confusion points or the **P**, **D**, and **T** JND values.

Chromaticities were defined in their location on a MacLeod-Boynton diagram [4] based on *L*, *M*, and *S* cone excitations. Cone excitations were calculated by multiplying the Stockman and Sharpe [25, 28] 2° cone fundamentals by the spectral power distribution of the primary colors of the CRT display in *P*, *D* and *T* points and the corresponding reference points. Cone fundamentals were scaled to provide that $L(\lambda) + M(\lambda)$ is equal to the luminosity function and that $S(\lambda)$ peaks at unity [6]. S' and L' coordinates of the MacLeod-Boynton diagram were calculated as $S/(L + M)$ and $L/(L + M)$, respectively.

The gamut of the display and the reference chromaticities are shown in Fig. 14.

Fig. 15 shows a reference point with the corresponding *P*, *D*, and *T* points and the Tritan, Protan, and Deutan confusions lines.

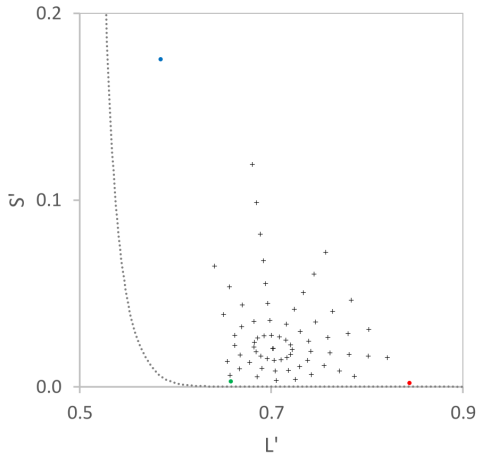

Fig. 14 The gamut of the display and the reference chromaticities in the MacLeod-Boynton chromaticity diagram. The dashed curve shows part of the spectrum locus of monochromatic lights.

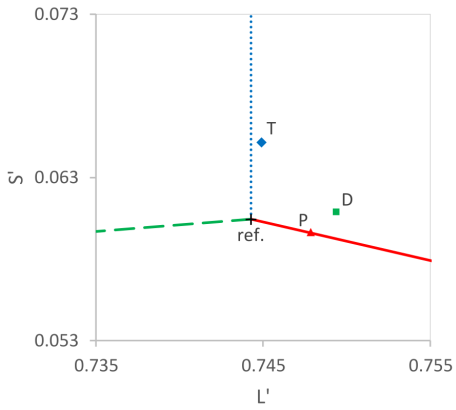

Fig. 15 The reference point −5 in reference direction (5) with the corresponding *P* (triangle), *D* (square), and *T* (diamond) values and the Protan (solid), Deutan (dashed), and Tritan (dotted) confusion lines in the MacLeod-Boynton diagram

T values represented in the MacLeod-Boynton diagram run mainly along with the S' ordinate, therefore $\Delta L'$ were disregarded in further analysis, and $\Delta S'$ was estimated as the differences between *T*'s ordinates and the reference point.

$\Delta L'$ was calculated as the Euclidean distance between *P* and the reference point. *P* and *D* values were evaluated only in terms of $\Delta L'$, and T values were evaluated only in terms of $\Delta S'$.

3.2.2 Threshold vs. reference stimulus (TVR)

Data plotted as threshold versus reference stimulus follows results presented in the literature showing that chromatic discrimination is best near the chromaticity of the surround. The log $\Delta S'$ and log $\Delta L'$ thresholds were plotted against log S' and log L' values, respectively in Figs. 16 and 17.

Data shows the asymmetrical V-shapes as reported by Smith and Pokorny [3, 6].

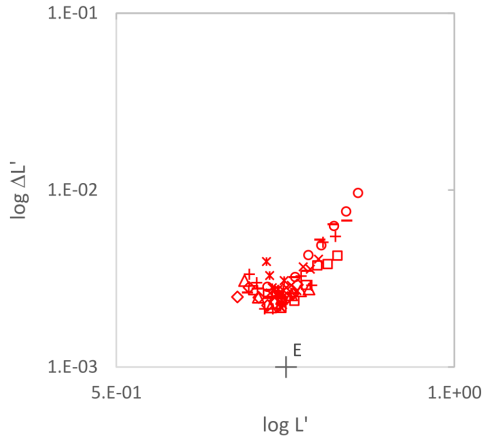

Fig. 16 The log $\Delta L'$ values plotted versus log L' reference stimuli. Different markers show data corresponding to the eight measurement directions as well as in Fig. 18. The grey cross indicates the L' chromaticity coordinate of equal energy white "*E*".

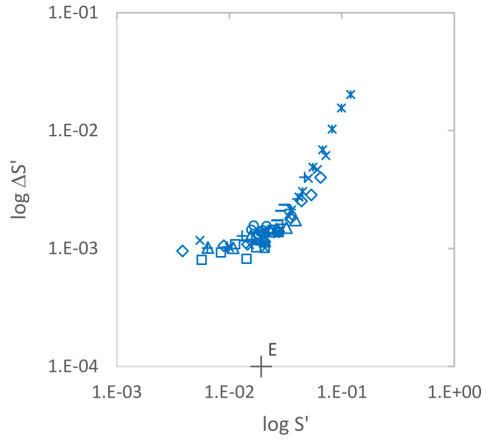

Fig. 17 The log $\Delta S'$ values plotted versus log S' reference stimuli. Different markers show data corresponding to the eight measurement directions as well as in Fig. 19. The grey cross indicates the L' chromaticity coordinate of equal energy white "*E*".

In our case, the minimum values of the V-shapes estimate well the S' and L' chromaticities of the equal energy white "E" ($S'_E = 0.0192$ and $L'_E = 0.7078$). Since measurements were executed in a dark room, the spectral power distribution of the surround was considered as equal energy in the whole visible wavelength range.

3.2.3 Cone excitations vs. $\Delta E_{u'v'}$

Figs. 18 and 19 show $\Delta L'$ and $\Delta S'$ values, respectively, as a function of reference point locus in the CIE 1976 UCS diagram (see left ordinates) and the plots of Figs. 7 and 8 in the background (see right ordinates).

Correlation analysis shows strong, positive, linear relationship between the **P**-$\Delta L'$, **D**-$\Delta L'$, and **T**-$\Delta S'$ datasets, towards the relevant confusion directions. The strength and the significance of the relationship vary in the different measurement directions. Spearman's correlation coefficients and the corresponding p-values between the averages of the datasets and the **P**-$\Delta L'$, **D**-$\Delta L'$, and **T**-$\Delta S'$ data respectively, towards the eight measurement directions are shown in Table 3.

The significant correlations indicate that the increase of the JNDs towards the confusion points expressed in $\Delta E_{u'v'}$ units does not only describe the non-uniformity of the CIE 1976 UCS diagram but shows a physiological phenomenon which can be revealed even in terms of cone excitations.

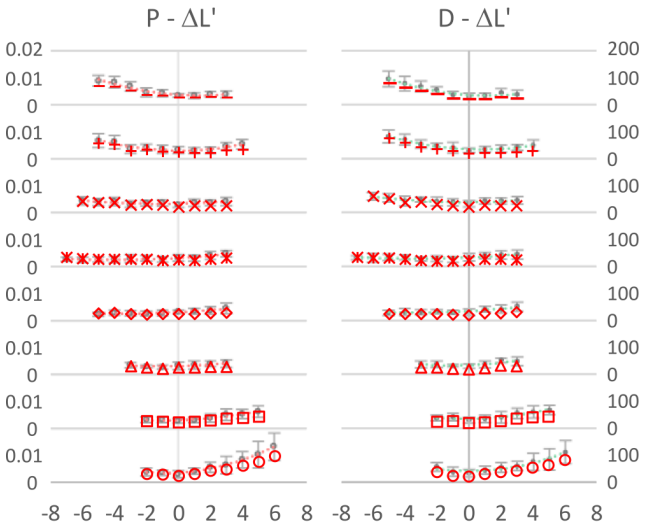

Fig. 18 The $\Delta L'$ values plotted on Fig. 7 as a function of the reference point location in the CIE 1976 UCS diagram. The abscissa is the ordinal number of reference points. Data is shown for reference directions from (0) to (7) as in Fig. 7. The right ordinates represent the distances within the CIE 1976 UCS diagram multiplied by 10^4, the scales of the subplots are 0–200. The left ordinates represent $\Delta L'$ values; the scales of the subplots are 0–0.02.

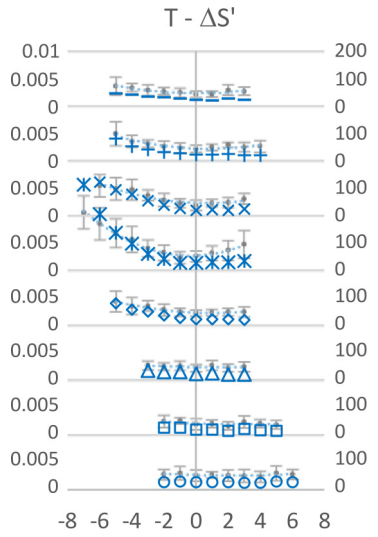

Fig. 19 The $\Delta S'$ values (diamonds) plotted on Fig. 8 as a function of the reference point location in the CIE 1976 UCS diagram. The abscissa is the ordinal number of reference points. Data is shown for reference directions from (0) to (7) as in Fig. 8. The right ordinates represent the distances within the CIE 1976 UCS diagram multiplied by 10^4, the scales of the subplots are 0–200. The left ordinates represent $\Delta L'$ values; the scales of the subplots are 0–0.01.

Table 3 Spearman correlation coefficients and p-values describing the relationship between the average JNDs and the **P**-$\Delta L'$, **D**-$\Delta L'$ and **T**-$\Delta S'$ data, respectively.

	Protan **P**-$\Delta L'$		Deutan **D**-$\Delta L'$		Tritan **T**-$\Delta S'$	
	Corr. coeff.	p-value	Corr. coeff.	p-value	Corr. coeff.	p-value
(7)	0.99	0.0000	0.98	0.0000	0.93	0.0002
(6)	0.99	0.0000	0.94	0.0158	0.65	0.0425
(5)	0.60	0.0667	0.73	0.0158	0.92	0.0002
(4)	-0.10	0.7456	0.31	0.3306	0.96	0.0000
(3)	0.48	0.1875	0.87	0.0025	0.72	0.0298
(2)	0.75	0.0522	0.88	0.0085	0.75	0.0522
(1)	0.99	0.0000	0.99	0.0000	0.88	0.0039
(0)	0.99	0.0000	0.98	0.0000	0.98	0.0000

4 Conclusion

Chromatic discrimination thresholds strongly depend on the relation between the observed stimuli and the state of chromatic adaptation [29]. Conversely, if we would like to describe chromatic discrimination thresholds under an actual state of chromatic adaptation, chromaticities close to the adapted white and far from the adapted white should be considered separately.

Krauskopf and Gegenfurtner [29] recommends that the best discriminability can be achieved when the observer is adapted to the discriminanda, or (in case of multiple discriminable colors) to the center of all colors perceived.

This approach can be helpful if the state of adaptation is adjustable, even though this is not always achievable and a converse approach is needed, where the viewing conditions (including the state of adaptation) are fixed, and chromatic discrimination thresholds should be observed accordingly.

We aimed to execute measurements with CCT covering the whole gamut of a display to provide normative values of JNDs in terms of reference chromaticity and to analyze the discrimination thresholds expressed in the CIE 1976 UCS diagram and in terms of cone excitations.

In order to cover a broad gamut covered with the reference points, display luminance levels were set to 5 ±3 cd/m^2, which is not only lower than the luminance values recommended in the CCT manual [17] but approximates the upper limit of the mesopic luminance range based on visual performance (0.005 cd/m^2 to 5 cd/m^2) proposed in the corresponding CIE document [30]. Vision under mesopic conditions is a topic of research from many aspects [31]. Rod activation even in daylight conditions was studied and reported [32]. A study of Walkey et al. [33] observing chromatic sensitivity in the mesopic range concluded that although chromatic discrimination thresholds increase towards the tritan confusion line by the reduction of luminance, chromatic discrimination may not be impaired by rod activation in a foveal and near-peripherical visual field. Adding that our measurements were obtained at the upper limit of the mesopic luminance range, we assumed that the reduced display luminance levels and the dark room might increase variability but did not expect changes in the measured JNDs caused by the activated rod-cone interactions. Our findings with the Cambridge Colour Test correspond well with the data found in the literature near the neutral reference point. However, extending the range of reference points in terms of chromaticity, our data shows that shifting the reference point towards the Protan, Deutan, or Tritan confusion points provides an increase of Just Noticeable Differences following second-order polynomials. A mathematical model and normative parameters are proposed to estimate the JNDs.

Shifting the chromaticity with approximately $\Delta E_{u'v'}$ = 0.13 JNDs measured towards the concerned confusion points of color-normal subjects exceed the threshold of color-normal subjects published in the CCT manual [17] and the shift of approximately $\Delta E_{u'v'}$ = 0.10 indicated JNDs above the normative thresholds found in the literature [26].

Results of pilot measurements showed that shifts towards saturation but not towards confusion points did not affect results significantly. Further measurements and analysis are required, but these initial results indicate that evaluation in terms of saturation does not necessarily provide enough information to predict changes in discrimination thresholds.

The isolated mechanism of short-wavelength-sensitive cones and the dependence between the middle-wavelength-sensitive and the long-wavelength-sensitive cones can be detected in the results. Analysis shows a high correlation between Protan and Deutan results in each direction. Tritan results correlate well with the others only in directions of purple-green chromaticities, which are not approximating any of the confusion lines running from the neutral point.

Results given in $L' = L/(L + M)$ and $S' = S/(L + M)$ MacLeod-Boynton chromaticity coordinates based on cone excitations follow the expected pattern: JNDs run along the corresponding confusion lines from the reference points, confirming the methods of CCT.

Threshold vs. reference stimulus plots in terms of L' and S' values follow the asymmetrical V-shape published by Smith and Pokorny [3, 6]. The abscissa of the minimal value of the V-shapes approximates the L' and S' chromaticity coordinates of the equal energy white "E", which corresponds to the surround of the measurement executed in a dark room [34, 35].

JNDs in $\Delta E_{u'v'}$ and $\Delta L'$ and $\Delta S'$ metrics were compared. **T** and $\Delta S'$ values correlate well towards bluish colors, which approximates the Tritan confusion line. Both **P** and **D** values correlate well with ΔL in the red-green direction, which approximates Protan and Deutan confusion lines.

The measured JNDs show similar pattern in the two color metrics, indicated by cone-excitations even towards reference directions in which significant correlation cannot be shown.

Although Just Noticeable Differences show similar patterns in the two color metrics, analysis in terms of the CIE 1976 UCS diagram does not necessarily provide enough information to predict changes in chromatic discrimination thresholds. Interpretation of data considering cone-excitations is recommended.

Acknowledgement

The research reported in this paper and carried out at BME has been supported by the NRDI Fund (TKP2020 IES, Grant No. BME-IE-BIO) based on the charter of bolster issued by the NRDI Office under the auspices of the Ministry for Innovation and Technology.

The research reported in this paper and carried out at BME has been supported by the NRDI Fund (TKP2020

NC, Grant No. BME-NC) based on the charter of bolster issued by the NRDI Office under the auspices of the Ministry for Innovation and Technology.

Authors thank all subjects who participated in the measurements for their contribution.

References

[1] Fairchild, M. D. "Color Appearance Models", John Wiley & Sons, Ltd, Hoboken, NJ, USA, 2013. https://doi.org/10.1002/9781118653128

[2] Kaiser, P. K., Boynton, R. M. "Human Color Vision", Optical Society of America, Washington, DC., USA, 1996.

[3] Smith, V. C., Pokorny, J. "3 - Color Matching and Color Discrimination", In: Shevell, S. K. (ed.) The Science of Color, Optical Society of America, Washington, DC., USA, 2003, pp. 103–148. https://doi.org/10.1016/B978-044451251-2/50004-0

[4] MacLeod, D. I. A., Boynton, R. M. "Chromaticity diagram showing cone excitation by stimuli of equal luminance", Journal of the Optical Society of America, 69(8), pp. 1183–1186, 1979. https://doi.org/10.1364/JOSA.69.001183

[5] Cole, G. R., Hine, T. "Computation of cone contrasts for color vision research", Behavior Research Methods, Instruments, & Computers, 24(1), pp. 22–27, 1992. https://doi.org/10.3758/BF03203465

[6] Smith, V. C., Pokorny, J. "The design and use of a cone chromaticity space: A tutorial", Color Research and Application, 21(5), pp. 375–383, 1996. https://doi.org/10.1002/(SICI)1520-6378(199610)21:5<375::AID-COL6>3.0.CO;2-V

[7] Danilova, M. V., Mollon, J. D. "Cardinal axes are not independent in color discrimination", Journal of the Optical Society of America A, 29(2), pp. A157–A164, 2012. https://doi.org/10.1364/josaa.29.00a157

[8] Krauskopf, J., Williams, D. R., Heeley, D. W. "Cardinal directions of color space", Vision Research, 22(9), pp. 1123–1131, 1982. https://doi.org/10.1016/0042-6989(82)90077-3

[9] MacAdam, D. L. "Visual Sensitivities to Color Differences in Daylight", Journal of the Optical Society of America, 32(5), pp. 247–274, 1942. https://doi.org/10.1364/JOSA.32.000247

[10] Le Grand, Y. "Les Seuils Différentiels de Couleurs dans la Théorie de Young" (The Differential Thresholds of Colors in Young's Theory), Archives d'Ophtalmologie et Revue Generale d'Ophtalmologie, 28(5), pp. 261–278, 1949. (in French)

[11] Boynton, R. M., Knoblauch, K. "Color difference thresholds in young's theory", Color Research and Application, 19(4), pp. 296–309, 1994. https://doi.org/10.1002/col.5080190410

[12] Nagy, A. L., Eskew, R. T., Boynton, B. M. "Analysis of color-matching ellipses in a cone-excitation space", Journal of the Optical Society of America A, 4(4), pp. 756–768, 1987. https://doi.org/10.1364/josaa.4.000756

[13] Kawamoto, K., Inamura, T., Yaguchi, H., Shioiri, S. "Color Discrimination Characteristics Depending on the Background Color in the (L, M) Plane of a Cone Space", Optical Review, 10(5), pp. 391–397, 2003. https://doi.org/10.1007/s10043-003-0391-2

[14] Ishihara, S. "Tests for color blindness", Kanehara Shuppan Co. Ltd., Tokyo, Kyoto, Japan, 1972.

[15] Regan, B. C., Reffin, J. P., Mollon, J. D. "Luminance noise and the rapid-determination of discrimination ellipses in color deficiency", Vision Research, 34(10), pp. 1279–1299, 1994. https://doi.org/10.1016/0042-6989(94)90203-8

[16] Hasrod, N., Rubin, A. "Colour vision: A review of the Cambridge Colour Test and other colour testing methods", African Vision and Eye Health, 74(1), Article number: 23, 2015. https://doi.org/10.4102/aveh.v74i1.23

[17] Mollon, J. D., Regan, B. C. "Cambridge Colour Test: Handbook", Cambridge Research Systems Ltd., Rochester, Kent, UK,2000.

[18] Regan, B. C., Mollon, J. D. "Discrimination ellipses in the MacLeod-Boynton diagram: Results for normal and colour-deficient subjects obtained with a CRT display", In: Drum, B., Adams, A. J., Cavonius, C. R., Dain, S. J., Haegerstrom-Portnoy, G., Kitahara, K., …, Zrenner, E. (eds.) Colour Vision Deficiencies XII, Springer, Dordrecht, Netherlands, 1995, pp. 445–451. https://doi.org/10.1007/978-94-011-0507-1_52

[19] Costa, M. F., Ventura, D. F., Perazzolo, F., Murakoshi, M., De Lima Silveira, L. C. "Absence of binocular summation, eye dominance, and learning effects in color discrimination", Visual Neuroscience, 23(3–4), pp. 461–469, 2006. https://doi.org/10.1017/S095252380623311X

[20] Paramei, G. V. "Color discrimination across four life decades assessed by the Cambridge Colour Test", Journal of the Optical Society of America A, 29(2), pp. A290–A297, 2012. https://doi.org/10.1364/JOSAA.29.00A290

[21] Paramei, G. V., Oakley, B. "Variation of color discrimination across the life span", Journal of the Optical Society of America A, 31(4), pp. A375–A384, 2014. https://doi.org/10.1364/JOSAA.31.00A375

[22] Shinomori, K., Panorgias, A., Werner, J. S. "Discrimination thresholds of normal and anomalous trichromats: Model of senescent changes in ocular media density on the Cambridge Colour Test", Journal of the Optical Society of America A, 33(3), pp. A65–A76, 2016. https://doi.org/10.1364/JOSAA.33.000A65

[23] Ventura, D. F., Silveira, L. C. L., Nishi, M., Costa, M. F., Gualtieri, M., dos Santos, R. M. A., ..., de Souza, J. M. "Perdas na visão de cores em pacientes tratados com cloroquina" (Color vision loss in patients treated with chloroquine), Arquivos Brasileiros de Oftalmologia, 66(5suppl), pp. 9–15, 2003. (in Spanish) https://doi.org/10.1590/s0004-27492003000600002

[24] Ventura, D. F., Simões, A. L., Tomaz, S., Costa, M. F., Lago, M., Costa, M. T. V., ..., Silveira, L. C. L. "Colour vision and contrast sensitivity losses of mercury intoxicated industry workers in Brazil", Environmental Toxicology and Pharmacology, 19(3), pp. 523–529, 2005. https://doi.org/10.1016/j.etap.2004.12.016

[25] Stockman, A., Sharpe, L. T. "The spectral sensitivities of the middle- and long-wavelength-sensitive cones derived from measurements in observers of known genotype", Vision Research, 40(13), pp. 1711–1737, 2000. https://doi.org/10.1016/S0042-6989(00)00021-3

[26] Ventura D. F., Silveria, L. C. L., Rodrigues, A. R., De Souza, J. M., Gualiteri, M., Bonci, D., Costa, M. F. "Preliminary Norms for the Cambridge Colour Test", In: Mollon, J. D., Pokorny, J., Knoblauch, K. (eds.) Normal and Defective Colour Vision, Oxford Scholarship Online, Oxford, UK, 2010, pp. 333–339. https://doi.org/10.1093/acprof:oso/9780198525301.003.0034

[27] Schanda, J. (ed.) "Colorimetry: Understanding the CIE System", John Wiley & Sons, Inc., Hoboken, NJ, USA, 2007. https://doi.org/10.1002/9780470175637

[28] Stockman, A., Sharpe, L. T., Fach, C. "The spectral sensitivity of the human short-wavelength sensitive cones derived from thresholds and color matches", Vision Research, 39(17), pp. 2901–2927, 1999. https://doi.org/10.1016/S0042-6989(98)00225-9

[29] Krauskopf, J., Gegenfurtner, K. "Color discrimination and adaptation", Vision Research, 32(11), pp. 2165–2175, 1992. https://doi.org/10.1016/0042-6989(92)90077-V

[30] International Commission on Illumination "Recommended System for Mesopic Photometry based on Visual Performance", International Commission on Illumination, Vienna, Austria, Rep. CIE 191:2010, 2010.

[31] Zele, A. J., Cao, D. "Vision under mesopic and scotopic illumination", Frontiers in Psychology, 5, Article number: 1594, 2015. https://doi.org/10.3389/fpsyg.2014.01594

[32] Tikidji-Hamburyan, A., Reinhard, K., Strochi, R., Dietter, J., Seitter, H., Davis, K. E, …, Münch, T. A. "Rods progressively escape saturation to drive visual responses in daylight conditions", Nature Communications, 8(1), Article number: 1813, 2017. https://doi.org/10.1038/s41467-017-01816-6

[33] Walkey, H. C., Barbur, J. L., Harlow, J. A., Makous, W. "Measurements of chromatic sensitivity in the mesopic range", Color Research and Application, 26(S1), pp. S36–S42, 2001. https://doi.org/10.1002/1520-6378(2001)26:1+<::aid-col9>3.0.co;2-s

[34] Zaidi, Q., Shapiro, A., Hood, D. "The Effect of Adaptation on the Differential Sensitivity of the *S*-cone Color System", Vision Research, 32(7), pp. 1297–1318, 1992. https://doi.org/10.1016/0042-6989(92)90224-7

[35] Miyahara, E., Smith, V. C., Pokorny, J. "How surrounds affect chromaticity discrimination", Journal of the Optical Society of America A, 10(4), pp. 545–553, 1993. https://doi.org/10.1364/josaa.10.000545